Original Article

Changes in crystalline lens parameters during accommodation evaluated using swept source anterior segment optical coherence tomography

Lanhua Wang[#], Guangming Jin[#], Xiaoting Ruan, Xiaoxun Gu, Xiaoyun Chen, Wei Wang, Ye Dai, Zhenzhen Liu, Lixia Luo

State Key Laboratory of Ophthalmology, Zhongshan Ophthalmic Center, Sun Yat-sen University, Guangdong Provincial Key Laboratory of Ophthalmology and Visual Science, Guangdong Provincial Clinical Research Center for Ocular Diseases, Guangzhou, China

Contributions: (I) Conception and design: L Luo, Z Liu; (II) Administrative support: L Luo, Z Liu; (III) Provision of study materials or patients: L Wang, G Jin; (IV) Collection and assembly of data: X Gu, X Ruan; (V) Data analysis and interpretation: L Wang, G Jin; (VI) Manuscript writing: All authors; (VII) Final approval of manuscript: All authors.

[#]These authors contributed equally to this work.

Correspondence to: Prof. Lixia Luo, MD, PhD; Prof. Zhenzhen Liu, MD, PhD. State Key Laboratory of Ophthalmology, Zhongshan Ophthalmic Center, Sun Yat-sen University, Guangzhou, China. Email: luolixia@gzzoc.com; liuzhenzhen@gzzoc.com.

Backgrounds: To assess changes in anterior segment biometry during accommodation using a swept source anterior segment optical coherence tomography (SS-OCT).

Methods: One hundred-forty participants were consecutively recruited in the current study. Each participant underwent SS-OCT scanning at 0 and −3 diopter (D) accommodative stress after refractive compensation, and ocular parameters including anterior chamber depth (ACD), anterior and posterior lens curvature, lens thickness (LT) and lens diameter were recorded. Anterior segment length (ASL) was defined as ACD plus LT. Lens central point (LCP) was defined as ACD plus half of the LT. The accommodative response was calculated as changes in total optical power during accommodation.

Results: Compared to non-accommodative status, ACD (2.952±0.402 *vs.* 2.904±0.382 mm, P<0.001), anterior (10.771±1.801 *vs.* 10.086±1.571 mm, P<0.001) and posterior lens curvature (5.894±0.435 *vs.* 5.767±0.420 mm, P<0.001), lens diameter (9.829±0.338 *vs.* 9.695±0.358 mm, P<0.001) and LCP (4.925±0.274 *vs.* 4.900±0.259 mm, P=0.010) tended to decreased and LT thickened (9.829±0.338 *vs.* 9.695±0.358 mm, P<0.001), while ASL (6.903±0.279 *vs.* 6.898±0.268 mm, P=0.568) did not change significantly during accommodation. Younger age (β=0.029, 95% CI: 0.020 to 0.038, P<0.001) and larger anterior lens curvature (β=−0.071, 95% CI: −0.138 to −0.003, P=0.040) were associated with accommodation induced greater steeping amplitude of anterior lens curvature. The optical eye power at 0 and −3 D accommodative stress was 62.486±2.284 and 63.274±2.290 D, respectively (P<0.001). Age was an independent factor of accommodative response (β=−0.027, 95% CI: −0.038 to −0.016, P<0.001).

Conclusions: During −3 D accommodative stress, the anterior and posterior lens curvature steepened, followed by thickened LT, fronted LCP and shallowed ACD. The accommodative response of −3 D stimulus is age-dependent.

Keywords: Accommodation; accommodative response; lens parameters; anterior lens curvature; posterior lens curvature

Received: 29 December 2021; Accepted: 26 August 2022; Published: 15 December 2022.

doi: 10.21037/aes-21-70

View this article at: https://dx.doi.org/10.21037/aes-21-70

Introduction

Accommodation is a dynamic process of retinal defocus when the eye focuses at different distances (1). Loss of accommodation due to presbyopia or cataract surgery is one of the most common complaints in ophthalmic patients. Although many basic and clinical researches were conducted (2,3), the mechanism of accommodation and presbyopia are not fully understood, and restoring accommodation remains a challenging task.

The lenticular changes mediated by ciliary muscle and zonule is commonly regarded as a key factor for accommodation and presbyopia (4-6). Loss of deformity of the lens with age is hypothesized to be the primary etiology of presbyopia (4). Thus, a detailed knowledge of the structural changes of the crystalline lens and optical properties during accommodation is of great importance in understanding the mechanism of accommodation and exploring new techniques for restoring dynamic accommodation. Additionally, exact data of dynamic changes amplitude in anterior chamber depth (ACD) and anterior lens position can help to assess the security of the implantable Collamer lens (ICL) which may cause cataract formation due to contact between the ICL and crystalline lens (7). Previous measurements of crystalline lens *in vivo* were mainly performed with A-scan (8), IOLmaster (9), Purkinje imaging (10), Scheimpflug camera (11), slit-lamp photography (12), ultrasound biomicroscopy (UBM) (13), or magnetic resonance imaging (MRI) (14). These measurements of the crystalline lens, however, were indirect measures with or without complexity of obtaining cross-sectional images, with limited visibility of the posterior lens surface, and debatable reproducibility and accuracy (12).

Anterior segment optical coherence tomography (AS-OCT) is a non-invasive method that offers high-resolution imaging of the anterior segment structures with high-speed, 3D imaging capability and providing coaxial accommodative targets which enables *in vivo* and real-time assessment of accommodation, and thus has gained wide used in clinical application to assess parameters of the anterior chamber angle, as well as accommodation due to its advantage of dynamic measurement (2,15,16). However, challenge exists to assess the entire crystalline lens in a single frame by commercial AS-OCT due to the limited scan depth and the sensitivity decay with depth. Currently, available methods to image the entire anterior segment with AS-OCT were obtained by complex phase-splitting techniques for conjugate removal (17), dual channel dual focus AS-OCT devices (18) or by overlapping images acquired at different depths (16), the reliability of which needs to be further assessed. Furthermore, the complexity of the techniques limited the possibility to generalize it in larger population-based studies.

In recent years, with the improved scan rate, scan depth, and scan density of the second generation swept source AS-OCT (SS-OCT) (CASIA2, TOMEY, Japan), it is now possible to obtain imaging from the cornea to the posterior lens surface in one cross-sectional image. The reliability and repeatability of CASIA2 in measuring anterior segment structures was high (19). Current studies of accommodation using CASIA2 are scarce (20-24). Therefore, we aimed to characterize changes in lens parameters and other anterior segment parameters including ACD, anterior segment length (ASL) and its associations using CASIA2 during −3 diopter (D) accommodative stress. We present the following article in accordance with the STROBE reporting checklist (available at https://aes.amegroups.com/article/view/10.21037/aes-21-70/rc).

Methods

Participants

One hundred-fifty-nine participants were consecutively recruited to participant in the current study from Aug 22 to Sep 10, 2019 at Zhongshan Ophthalmic Center (ZOC), southern China. Exclusion criterion were best corrected Visual Acuity (BCVA) of less than 20/20; previous history of ocular disease or surgeries; history of wearing contact lenses; anterior segment abnormality; poor quality SS-OCT images; or inability to cooperate during examination. The study was conducted in accordance with the Declaration of Helsinki (as revised in 2013). Ethical approval was obtained from the Zhongshan University Ethics Review Board (No. 2019KYPJ033). Written informed consent was obtained from all participants.

Ocular examinations

All participants underwent uncorrected visual acuity (UCVA) and BCVA examination using an Early Treatment Diabetic Retinopathy Study (ETDRS) visual chart at a distance of 4 m. Non-cycloplegic refractions were measured by an autorefractor (KR8800; Topcon, Tokyo, Japan). The refraction data were further converted to spherical equivalent (SE) which was defined as spherical power plus half of the

cylindrical power. Axial length (AL) was measured by an optical biometer (IOLmaster700, Carl Zeiss Meditec, Jena, Germany). A slit lamp examination was adapted to detect abnormalities of the anterior and posterior segments. Each examination was performed by the same experienced nurse by a standard protocol to ensure reliability.

SS-OCT examinations

The SS-OCT device (CASIA2, Tomey Corporation, Nagoya, Japan) with a laser wavelength of 1,310 nm was used to obtain images of the anterior segment before and during accommodation. All measurements were conducted under a standard procedure in a darkened room with the same device settings by the same research nurse. SS-OCT scans of the lens analysis model were obtained at the accommodative resting state and at an accommodative stress on –3 D after refractive compensation by a build-in system of the CASIA2. Before scanning, refractive error of the tested eye was corrected by the built-in system. The anterior segment images of the tested eye in unaccommodated state was captured with the participant focusing on the co-axial internal fixation target image set for distance in the CASIA2 device for the first 5 seconds. Afterward, –3.0 D accommodative stress by the built-in system of the CASIA2 was added to stimulate the physiologic accommodation, and images were captured when the participant could clearly look forward at the internal fixation target for 5 seconds. The eye was centered by the active eye tracker system in CASIA2. Corneal topographic axis, defined as a reference line connecting the fixation point in the topographer to the vertex normal on the cornea, was used as positional reference for comparative images obtained from the unaccommodated and accommodated states (25,26). To avoid eye movement, rotation, convergence or other movements during scanning, participants were guided to keep their jaw and forehead on the fixed trestle, while staring at the co-axial internal fixation target during scanning. Then the device automatically analyzed and displayed values of ACD, anterior and posterior lens curvature, lens thickness (LT) and lens diameter at 3-dimensional space. In order to ensure the reliability of the automatic results generated by the CASIA2, the "semi-auto" setting was used to check the accuracy of the automatic outline and re-modify the outline in scans with poorly automatically detected outlines. Three-dimensional data of the anterior segment parameters were analyzed. ACD was defined as the distance between the corneal epithelium and the anterior surface of the lens. ASL was defined as ACD plus LT. Lens central point (LCP) was defined as ACD plus half of the LT. The corneal model was used to obtain measurements of corneal power.

Accommodative response

The accommodative response was defined as changes in refractive power of the eye during accommodation based on a schematic eye model in paraxial approximation (Eq. [2]).

$$P_L = \left(n_l - n_h\right)\left(\frac{1}{R_a} - \frac{1}{R_p}\right) + \frac{\left(n_l - n_h\right)^2 LT}{n_l R_a R_p} \quad [1]$$

$$P = P_C + P_L - \frac{ACDP_C P_L}{n_h} + \frac{\left(n_l - n_h\right) LTP_C}{n_l R_p} \quad [2]$$

Where P, P_C *and* P_L refer to the power of the equivalent total eye, cornea and lens, respectively. Values of P_C were obtained from the CASIA2, n_l is the refractive index of the lens which is adjusted for age (27), n_h=1.336 is the refractive index of the aqueous humor, R_a and R_p represent the radius of anterior and posterior lens curvatures.

Statistical analysis

All statistical analyses were performed with Stata (ver. 12.0; Stata Corp., College Station, TX). All data were presented for right eyes. The Skewness-Kurtosis test and histogram were used to test the normality of variables. Continuous variables were presented as the mean ± standard deviation (SD) or median [interquartile range (IQR)]. Analysis of variance (ANOVA) for normal distributions, or the Kruskal Wallis test for very skewed distributions were used to compare anterior segment parameters between age groups. Changes in anterior segment parameters, including anterior lens curvature, posterior lens curvature, LT, lens diameter, ACD, LCP and ASL, were calculated by subtracting anterior segment parameters at the accommodative resting state from anterior segment parameters at –3 D accommodative stress. Paired *t*-test was used to test for changes in anterior segment parameters during –3 D accommodative stress. Univariate and multivariate regression models were used to determine associated factors with changes in anterior lens curvature, posterior lens curvature and accommodative response of –3 D accommodative stimulus. A P value of <0.05 was defined to indicate statistical significance.

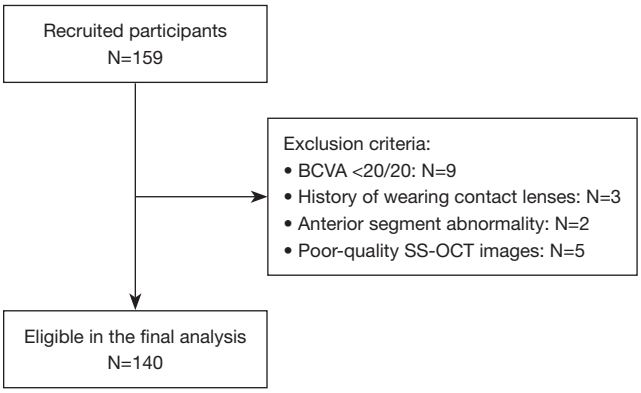

Figure 1 Flowchart of participants' selection. BCVA, best corrected visual acuity; SS-OCT, swept source optical coherence tomography.

Table 1 Distribution of basic characteristics among participants

Basic characteristic	Values
Participants, n	140
Age group, median (IQR)	30 (23 to 44)
10–20 years, n (%)	24 (17.14)
21–40 years, n (%)	68 (48.57)
41–59 years, n (%)	48 (34.29)
Male, n (%)	57 (40.71)
Female, n (%)	83 (59.29)
SE (D), median (IQR)	–1.13 (–4.13 to 0)
AL (mm), (mean ± SD)	24.28±1.52

IQR, interquartile range; SE, spherical equivalent; D, diopter; AL, axial length; SD, standard deviation.

Results

Of the 159 recruited participants, 19 were excluded due to having BCVA of less than 20/20 (9 participants), history of wearing contact lenses (3 participants), anterior segment abnormality (2 participants) and poor-quality SS-OCT images (5 participants), leaving 140 eligible participants for the final analysis (*Figure 1*). The distribution of basic characters of the included participants is presented in *Table 1*. In general, images of 140 participants with a median (IQR) age of 30 (23 to 44) years (age range, 10–59 years) and a male proportion of 40.71% were obtained under both the static state and at an accommodative amplitude of –3 D. The median (IQR) SE was –1.13 (–4.13, 0) D and the mean AL was 24.28±1.52 mm.

Table 2 presents result of changes in anterior segment biometry during –3 D accommodative stimulus by age groups. Compared to non-accommodative status, ACD (2.952±0.402 *vs.* 2.904±0.382 mm, P<0.001), anterior (10.771±1.801 *vs.* 10.086±1.571 mm, P<0.001) and posterior lens curvature (5.894±0.435 *vs.* 5.767±0.420 mm, P<0.001), lens diameter (9.829±0.338 *vs.* 9.695±0.358 mm, P<0.001) and LCP (4.925±0.274 *vs.* 4.900±0.259 mm, P=0.010) tended to decreased and LT thickened (9.829±0.338 *vs.* 9.695±0.358 mm, P<0.001), while ASL (6.903±0.279 *vs.* 6.898±0.268 mm, P=0.568) did not change significantly during accommodation. The changing amplitude of anterior lens curvature, posterior lens curvature, and LT tended to be smaller with increasing age (all P<0.05).

Table 3 shows the associated factors with changes in anterior and posterior lens curvature during –3 D accommodative stress. In the univariable model, participants who were younger (β=0.033, 95% CI: 0.025 to 0.041, P<0.001), female gender (β=0.411, 95% CI: 0.191 to 0.630, P<0.001), had myopic SE (β=0.083, 95% CI: 0.045 to 0.120, P<0.001), longer AL (β=–0.180, 95% CI: –0.258 to –0.101, P<0.001), deeper ACD (β=–0.778, 95% CI: –1.031 to –0.525, P<0.001), larger anterior (β=–0.189, 95% CI: –0.243 to –0.134, P<0.001) and posterior lens curvature (β=–0.399, 95% CI: –0.650 to –0.148, P=0.002), thinner LT (β=0.847, 95% CI: 0.619 to 1.074, P<0.001) and more backward of LCP (β=–0.655, 95% CI: –1.053 to –0.258, P=0.001) were more likely to have larger steeping of the anterior lens curvature after –3 D accommodative stimulus. Younger age (β=0.029, 95% CI: 0.020 to 0.038, P<0.001) and larger anterior (β=–0.071, 95% CI: –0.138 to –0.003, P=0.040) lens curvature were still associated with larger accommodation-induced steeping of the anterior lens curvature after adjusting for age, gender and SE. Younger age (β=0.004, 95% CI: 0.001 to 0.007, P=0.014) and larger posterior (β=–0.102, 95% CI: –0.184 to –0.021, P=0.014) lens curvature were associated with larger accommodation-induced steepening of posterior lens curvature after adjusting for confounders. There was a positive correlation between changes in anterior lens curvature and changes in posterior lens curvature (r=0.518, P<0.001) and lens diameter (r=0.743, P<0.001), ACD (r=0.847, P<0.001), and LCP (r=0.601, P<0.001), while changes in anterior lens curvature was negatively correlated with changes in LT (r=–0.881, P<0.001) and ASL (r=–0.387, P<0.001) (*Figure 2*). A similar correlation was also observed for changes in posterior lens curvature (*Figure 3*).

Table 2 Changes in the anterior segment biometry during accommodation stratified by age

Anterior segment biometrics	Total (n=140)	Age groups			P value
		10–20 years (n=24)	21–40 years (n=68)	41–59 years (n=48)	
ACD (mm)					
Non-accommodation status	2.952±0.402	3.235±0.314	3.059±0.330	2.647±0.356	<0.001
–3 D accommodation status	2.904±0.382	3.181±0.320	3.008±0.322	2.606±0.308	<0.001
Difference	–0.048±0.113	–0.054±0.037	–0.051±0.039	–0.041±0.190	0.856
P value	<0.001	<0.001	<0.001	0.167	
Anterior lens curvature (mm)					
Non-accommodation status	10.771±1.801	12.452±1.444	11.116±1.667	9.440±1.071	<0.001
–3 D accommodation status	10.086±1.571	11.279±1.584	10.194±1.551	9.288±1.060	<0.001
Difference	–0.684±0.720	–1.073±0.812	–0.922±0.708	–0.152±0.221	<0.001
P value	<0.001	<0.001	<0.001	0.010	
Posterior lens curvature (mm)					
Non-accommodation status	5.894±0.435	6.169±0.319	5.923±0.462	5.715±0.366	<0.001
–3 D accommodation status	5.767±0.420	5.984±0.308	5.778±0.452	5.643±0.380	0.004
Difference	–0.126±0.162	–0.185±0.130	–0.144±0.156	–0.072±0.171	0.008
P value	<0.001	<0.001	<0.001	0.006	
Lens thickness (mm)					
Non-accommodation status	3.962±0.421	3.488±0.153	3.843±0.304	4.369±0.275	<0.001
–3 D accommodation status	4.006±0.401	3.555±0.170	3.900±0.299	4.380±0.267	<0.001
Difference	0.043±0.045	0.068±0.047	0.057±0.043	0.011±0.027	<0.001
P value	<0.001	<0.001	<0.001	0.006	
Lens diameter (mm)					
Non-accommodation Status	9.829±0.338	9.784±0.256	9.804±0.365	9.886±0.332	0.342
–3 D accommodation Status	9.695±0.358	9.601±0.273	9.631±0.366	9.831±0.350	0.004
Difference	–0.134±0.135	–0.183±0.136	–0.173±0.134	–0.056±0.100	<0.001
P value	<0.001	<0.001	<0.001	<0.001	
LCP (mm)					
Non-accommodation status	4.925±0.274	4.976±0.283	4.975±0.247	4.822±0.287	0.014
–3 D accommodation status	4.900±0.259	4.957±0.282	4.953±0.243	4.789±0.239	0.002
Difference	–0.025±0.111	–0.019±0.17	–0.022±0.021	–0.033±0.191	0.854
P value	0.010	0.010	<0.001	0.261	
ASL (mm)					
Non-accommodation status	6.903±0.279	6.720±0.258	6.903±0.244	6.991±0.299	<0.001
–3 D accommodation status	6.898±0.268	6.734±0.255	6.903±0.246	6.969±0.275	0.002
Difference	–0.006±0.114	–0.013±0.18	–0.000±0.052	–0.022±0.183	0.417
P value	0.568	0.002	0.967	0.408	

All data presented as mean ±standard deviation. ACD, anterior chamber depth; LCP, lens central point; ASL, anterior segment length.

Table 3 Factors associated with changes in anterior and posterior lens curvature during −3 D accommodative stress

Characteristics	Anterior lens curvature				Posterior lens curvature			
	Model1 β		Model2 β		Model1 β		Model2 β	
	95% CI	P value	95% CI	P value	95% CI	P value	95% CI	P value
Age (years)	0.033 (0.025, 0.041)	<0.001	0.029 (0.020, 0.038)	<0.001	0.003 (0.001, 0.006)	0.006	0.004 (0.001, 0.007)	0.014
Female gender	0.411 (0.191, 0.630)	<0.001	0.157 (−0.040, 0.354)	0.118	0.077 (−0.013, 0.142)	0.020	0.065 (−0.003, 0.134)	0.007
SE (D)	0.083 (0.045, 0.120)	<0.001	0.010 (−0.029, 0.049)	0.604	0.013 (0.003, 0.022)	0.009	−0.007 (−0.020, 0.006)	0.287
AL (mm)	−0.180 (−0.258, −0.101)	<0.001			−0.020 (−0.046, 0.006)	0.135		
Anterior segment parameters (mm)								
ACD	−0.778 (−1.031, −0.525)	<0.001	−0.229 (−0.550, 0.092)	0.160	−0.097 (−0.177, −0.017)	0.018	−0.048 (−0.162, 0.065)	0.402
Anterior lens curvature	−0.189 (−0.243, −0.134)	<0.001	−0.071 (−0.138, −0.003)	0.040	−0.014 (−0.032, 0.004)	0.127	0.006 (−0.018, 0.030)	0.626
Posterior lens curvature	−0.399 (−0.650, −0.148)	0.002	−0.007 (−0.250, 0.236)	0.955	−0.131 (−0.202, −0.060)	0.001	−0.102 (−0.184, −0.021)	0.014
Lens thickness	0.847 (0.619, 1.074)	<0.001	0.117 (−0.291, 0.526)	0.570	0.090 (0.013, 0.166)	0.022	0.004 (−0.145, 0.137)	0.954
Lens diameter	−0.010 (−0.347, 0.327)	0.954	−0.165 (−0.454, 0.124)	0.261	−0.086 (−0.180, 0.008)	0.074	0.014 (−0.069, 0.096)	0.744
LCP	−0.655 (−1.053, −0.258)	0.001	−0.262 (−0.637, 0.114)	0.170	−0.094 (−0.211, −0.022)	0.110	−0.068 (−0.201, 0.065)	0.311
ASL	0.297 (−0.100, 0.695)	0.141	−0.200 (−0.568, 0.167)	0.283	0.010 (−0.104, 0.123)	0.869	−0.066 (−0.194, 0.062)	0.311

Model1: univariable regression model; Model2: adjusted for age, gender and SE. SE, spherical equivalent; D, diopter; AL, axial length; ACD, anterior chamber depth; LCP, lens central point; ASL, anterior segment length.

Changes in optical power of the whole eye and the isolated lens are calculated using Eqs. [1,2]. The optical power of the whole eye at 0 D and −3 D accommodative stress was 62.49±2.28 and 63.27±2.29 D, respectively (P<0.001). Accordingly, the lens power was 24.03±1.89 D at 0 D and which increased to 24.90±2.05 D during −3 D of accommodative stress (P<0.05). Younger age was associated with greater accommodative response (β=−0.027, 95% CI: −0.038 to −0.016, P<0.001) in the multivariable regression model (*Table 4*).

Discussion

The current study found that the anterior segment biometry including ACD, anterior lens curvature, posterior lens curvature, lens diameter, LCP and LT changed significantly during −3 D accommodative stress, while ASL did not change during accommodation. Participants with older age and smaller anterior lens curvature tended to have smaller decreasing amplitude of the anterior lens curvature during accommodation. The accommodative response of −3 D stimulus decreased with age. Previous studies on accommodation have been based on small study samples or based on traditional or compound imaging which cannot directly observe changes of the entire anterior segment, thus decreased reliability (13,14,16,18). To further understand the mechanism of accommodation and on-set of presbyopia and its related factors, studies of larger sample sizes with scans in which images are entirely visible are needed. To the best of our knowledge, this is so far the study containing

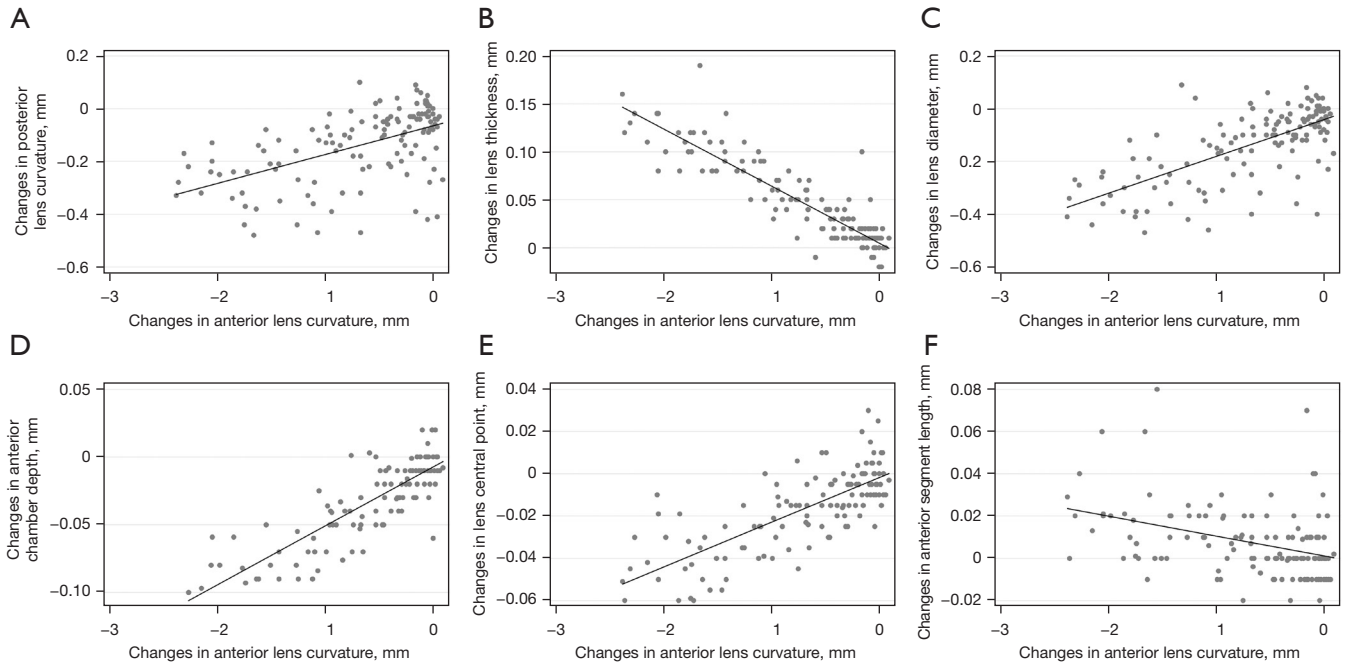

Figure 2 Correlation of changes in posterior lens curvature (A), lens thickness (B), lens diameter (C), anterior chamber depth (D), lens central point (E) and anterior segment length (F) with changes in anterior lens curvature.

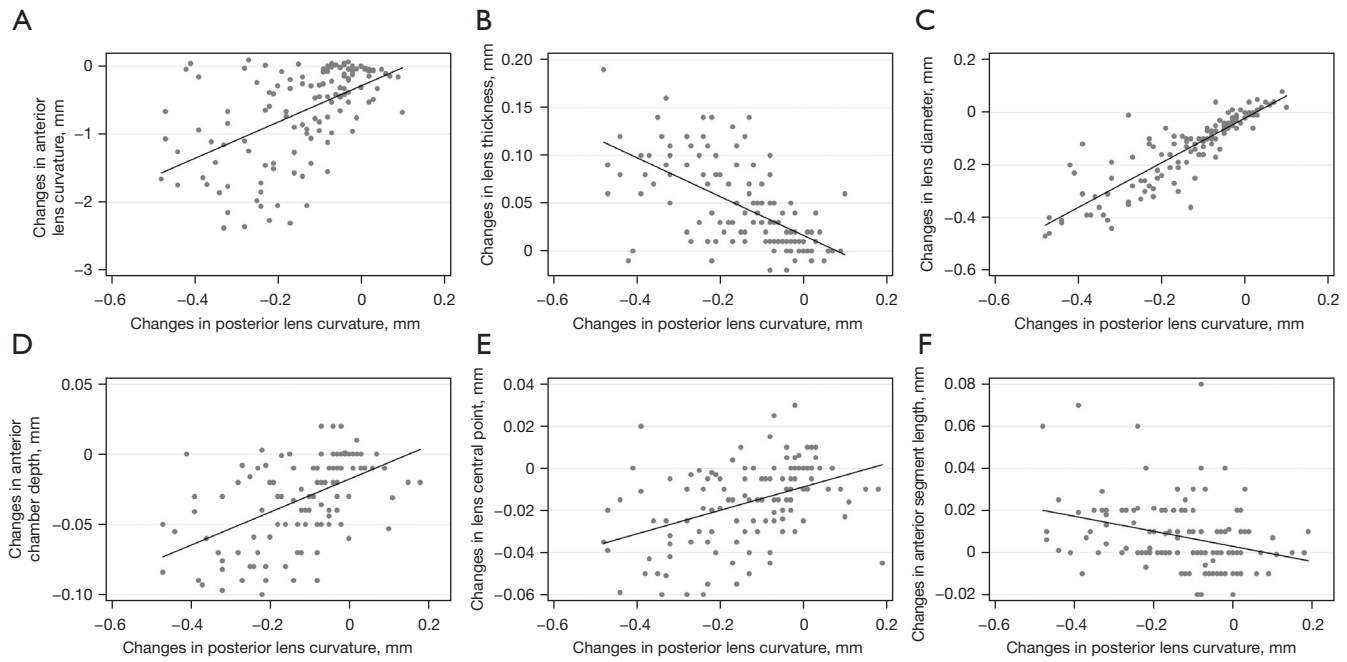

Figure 3 Correlation of changes in anterior lens curvature (A), lens thickness (B), lens diameter (C), anterior chamber depth (D), lens central point (E) and anterior segment length (F) with changes in posterior lens curvature.

Table 4 Factors associated with accommodative response during −3 D accommodative stress

Characteristics	Model1		Model2	
	β (95% CI)	P value	β (95% CI)	P value
Age (years)	−0.031 (−0.040, −0.022)	<0.001	−0.027 (−0.038, −0.016)	<0.001
Female gender	−0.337 (−0.584, −0.090)	0.008	−0.117 (−0.345, −0.110)	0.309
SE (D)	−0.090 (−0.133, −0.047)	<0.001	−0.023 (−0.069, 0.024)	0.333
AL (mm)	0.171 (0.081, 0.261)	<0.001		
Anterior segment parameters				
ACD (mm)	0.601 (0.397, 0.0.805)	<0.001	0.164 (−0.219, 0.546)	0.399
Anterior lens curvature (mm)	0.122 (0.056, 0.188)	<0.001	−0.034 (−0.114, 0.046)	0.404
Posterior lens curvature (mm)	0.298 (0.005, 0.591)	0.046	−0.154 (−0.429, 0.122)	0.272
Lens thickness (mm)	−0.740 (−1.013, −0.466)	<0.001	0.103 (−0.366, 0.571)	0.665
Lens diameter (mm)	−0.319 (−0.691, 0.052)	0.091	−0.221 (−0.558, 0.116)	0.197
LCP (mm)	0.715 (0.275, 1.156)	0.002	0.284 (−0.173, 0.740)	0.221
ASL	−0.128 (−0.582, 0.327)	0.580	0.318 (−0.127, 0.763)	0.160

Model1: univariable regression model; Model2: adjusted for age, gender and SE. SE, spherical equivalent; D, diopter; AL, axial length; ACD, anterior chamber depth; LCP, lens central point; ASL, anterior segment length.

the largest study sample by the CASIA2, the scanning depth of which enables us to obtain a single anterior segment image from anterior cornea to posterior lens surface and automatically generate data of anterior segment parameters with build-in software.

Our findings that lens curvature steepened followed by LT thickened and ACD shallowed are in accordance with the widely accepted Schachar mechanism (5,28-30). Accommodation-related decrease of anterior lens curvature, increase of LT and shallow of ACD have been well verified by numerous studies using Scheimpflug, AS-OCT, and other methods (2,14). However, lack of available methods for imaging the posterior lens curvature, most of which are currently obtained indirectly or through complex machine or overlapping images, limited our knowledge of accommodation-related changes in the posterior lens curvature. Some studies found a statistically significant reduction in posterior lens surface curvatures during accommodation using MRI (14) or SD-OCT (31), but other studies have indicated no changes (32,33). The possible reason for the controversy may be due to the low resolution of images and low reliability of the synthesized images. The enhanced penetration and speed of the CASIA2 enables the visibility of the entire anterior segment in one cross-sectional image in real-time and automatic analysis, which is a useful method in evaluating dynamic changes in lens parameters during accommodation. Our study indicated that posterior lens curvature steepened during −3 D accommodation. Current studies on accommodation using CASIA2 are scarce. One study of 30 participants aged 20 years and older from Japan presented preliminary values of anterior lens curvature, posterior lens curvature and LT before and after −3 D accommodative stress. However, it is difficult to determine whether changes in lens parameters during accommodation happened because this paper did not make statistical test for these changes (23). The same researchers did a more detailed analysis of accommodation-related changes in lens parameters in another study, with the results indicating that anterior and posterior lens curvatures steepened and LT thickened during accommodation in 96 included eyes, but the exact values of lens biometry were not presented (20). Thus, we cannot make direct comparison between our study and the aforementioned studies (20,23).

Studies on changes of the position of the posterior lens pole (ASL) during accommodation is controversial, with some studies having indicated no significant changes (16,34), but others found a significant backward-displacement of the posterior lens position (3,31). Variation of different measurements, or imaging length of technique may partly

explain these disparities. Our finding that ASL did not change with accommodation supports the Schachar theory that the lens position remains stable during accommodation (5,28).

Our and previous studies (14,35,36) indicate that the accommodation induces changes in anterior lens curvature is larger than the posterior lens curvature during –3 D accommodative stress. Additionally, the accommodation-induced changes in the amplitude and slope of the anterior lens curvature are different from the posterior lens curvature. One 3D MRI study showed that changes in anterior lens curvature were larger than those of posterior lens curvature, and changes in slope of the anterior and posterior lens curvature were not linear during accommodation (14). Gambra *et al.* (35) found that there was a decrease of 0.73 mm/D for the anterior lens curvature and 0.20 mm/D for the posterior lens curvature with increasing accommodative demand from 0 to 6 D by 1-D step. Results from an AS-OCT study indicated that changes in lens biometry were limited to the anterior lens curvature if accommodative stress was less than 1.5 D, while the posterior lens curvature was additionally altered in the process of accommodation only above the 1.5 D accommodative stress level (36). The reason for the differences in response of anterior and posterior lens curvatures to accommodation may be due to differences in insertion position and direction of the zonulas fiber or the relative position of the ciliary muscle to the lens (3).

The human lens, which provides one-third of the ocular optical power, is responsible for refocusing on targets at different distances through alteration of its shape to decrease or increase ocular optical power during accommodation. Previous studies showed that the deformability of the crystalline lens decreased with age, but the contractility of the muscle did not decline with age (2,27). One study using a combination of two SD-OCT systems to acquire synchronized images of the ciliary body and lens showed that accommodation-induced changes in LT was larger in younger subject, and younger subject had faster responses in the crystalline lens after contraction of the ciliary muscle (37). Richdale *et al.* (38) found that accommodative response increased linearly with increasing accommodation demand among subjects younger than 40 years but increased little among subjects aged 40 years and older; the lost rate of maximum accommodative response was 0.2 D/age. The current study found that the amplitude of reshaping of anterior and posterior lens curvatures during –3 D accommodative stimulus was significantly decreased with age, as well as the accommodative response which represents the real accommodative power under –3 D accommodative stimulus (0.027 D per year).

The mean value of –3 D accommodation-induced changes in ocular refractive power of the whole eye in our study was 0.79 D (range from –0.10 to 3.04 D), which is smaller than found in other studies. One OCT study of 4 subjects indicated that the changes of refractive power was about 3.8 D during 6 D accommodative demands (35). Another OCT study of 19 eyes from 13 subjects with a mean age of 28.6±4.4 years showed that the changes of refractive power was 4.14 D during 0–6 D accommodative demands in 1.5 D steps (31). Richdale *et al.* (38) found that the response amplitudes of 6 D accommodation were 0.03 to 5.15 D among 26 emmetropic adult aged 30 to 50 years using an auto-refractor. The relative wide age range in the current study may partly explain the difference. However, differences in measurement technique, study design, and race prohibited a direct comparison of our study with previous studies (31,35,38).

Strength of our study included the relatively large study sample size, standardize study protocol, and the new SS-OCT device which enable visibility of the entire lens figure and automatic analysis. Several limitations of the current study should be mentioned. First, analysis of some accommodation-related mechanisms including changes to ciliary muscle and zonular fibers were not available in the current study. Second, understanding accommodation-induced changes in lens surface area and lens volume, followed by refractive index (39-42) and crystalline lens density may help to provide a more in-depth understanding the mechanism of accommodation. However, currently available SS-OCT device cannot measure lens surface areas and lens volumes. Third, characteristics of lens biometry changes in other accommodative states than presently examined (>–3 D or maximum accommodative response) should be further assessed. Fourth, the fact that accommodative response was estimated by equation instead of auto-refractor which is an objective measurement of the accommodative response may have skewed our data. Compared to the equation of optical power, an indirect measurement, evaluating the accommodative response directly using an auto-refractor or other objective measurements may increase the reliability of the measurements. Fifth, the dynamic behavior of the lens during accommodation may potentially influence the accuracy of the measurements which were obtained only once at each status. Finally, it is difficulty to evaluate changes in equatorial diameter because the edge of the lens

cannot be visualized due to the presence of the iris by using AS-OCT (15,43). The lens diameter in the current study was obtained by fitting the anterior and posterior circular curves which may not exactly represent the real shape of the lens during accommodation.

In conclusion, the current study found that the lens is elastically deformed during accommodation which include steepening anterior and posterior lens curvature, decreased lens diameter and increased LT, followed by decreasing ACD and forward-displacement of LCP in almost all age subgroups. We found no significant changes in ASL in accommodation. Our findings support Schachar's accommodative hypotheses that the lens is stable during accommodation. The accommodative response of –3 D stimulus is age-dependent. These data may help us further understand the age-dependent mechanisms of accommodation.

Acknowledgments

Funding: This study was supported by the National Natural Science Foundation of China (Nos. 81770905 and 81873675) and the Construction Project of High-Level Hospitals in Guangdong Province (No. 303020102).

Footnote

Reporting Checklist: The authors have completed the STROBE reporting checklist. Available at https://aes.amegroups.com/article/view/10.21037/aes-21-70/rc

Data Sharing Statement: Available at https://aes.amegroups.com/article/view/10.21037/aes-21-70/dss

Conflicts of Interest: All authors have completed the ICMJE uniform disclosure form (available at https://aes.amegroups.com/article/view/10.21037/aes-21-70/coif). The authors have no conflicts of interest to declare.

Ethical Statement: The authors are accountable for all aspects of the work in ensuring that questions related to the accuracy or integrity of any part of the work are appropriately investigated and resolved. The study was conducted in accordance with the Declaration of Helsinki (as revised in 2013). Ethical approval was obtained from the Zhongshan University Ethics Review Board (No. 2019KYPJ033). Written informed consent was obtained from all participants.

References

1. Charman WN. Physiological optics in 2008: standing on Helmholtz's shoulders. Ophthalmic Physiol Opt 2009;29:209-10.
2. Shao Y, Tao A, Jiang H, et al. Age-related changes in the anterior segment biometry during accommodation. Invest Ophthalmol Vis Sci 2015;56:3522-30.
3. Bolz M, Prinz A, Drexler W, et al. Linear relationship of refractive and biometric lenticular changes during accommodation in emmetropic and myopic eyes. Br J Ophthalmol 2007;91:360-5.
4. von Helmholtz H. Uber die Akkommodation des Auges. Graefes Arch Clin Exp Ophthalmol 1855;1:1-89.
5. Schachar RA. Cause and treatment of presbyopia with a method for increasing the amplitude of accommodation. Ann Ophthalmol 1992;24:445-7, 452.
6. Wang K, Pierscionek BK. Biomechanics of the human lens and accommodative system: Functional relevance to physiological states. Prog Retin Eye Res 2019;71:114-31.
7. Lindland A, Heger H, Kugelberg M, et al. Vaulting of myopic and toric Implantable Collamer Lenses during accommodation measured with Visante optical coherence tomography. Ophthalmology 2010;117:1245-50.
8. He M, Huang W, Li Y, et al. Refractive error and biometry in older Chinese adults: the Liwan eye study. Invest Ophthalmol Vis Sci 2009;50:5130-6.
9. Ferrer-Blasco T, Esteve-Taboada JJ, Monsálvez-Romín D, et al. Ocular biometric changes with different accommodative stimuli using swept-source optical coherence tomography. Int Ophthalmol 2019;39:303-10.
10. Rosales P, Dubbelman M, Marcos S, et al. Crystalline lens radii of curvature from Purkinje and Scheimpflug imaging. J Vis 2006;6:1057-67.
11. Rosales P, Marcos S. Pentacam Scheimpflug quantitative imaging of the crystalline lens and intraocular lens. J Refract Surg 2009;25:421-8.
12. Schaeffel F. Binocular lens tilt and decentration

measurements in healthy subjects with phakic eyes. Invest Ophthalmol Vis Sci 2008;49:2216-22.
13. Mora P, Sangermani C, Ghirardini S, et al. Ultrasound biomicroscopy and iris pigment dispersion: a case--control study. Br J Ophthalmol 2010;94:428-32.
14. Sheppard AL, Evans CJ, Singh KD, et al. Three-dimensional magnetic resonance imaging of the phakic crystalline lens during accommodation. Invest Ophthalmol Vis Sci 2011;52:3689-97.
15. Du C, Shen M, Li M, et al. Anterior segment biometry during accommodation imaged with ultralong scan depth optical coherence tomography. Ophthalmology 2012;119:2479-85.
16. Neri A, Ruggeri M, Protti A, et al. Dynamic imaging of accommodation by swept-source anterior segment optical coherence tomography. J Cataract Refract Surg 2015;41:501-10.
17. Jungwirth J, Baumann B, Pircher M, et al. Extended in vivo anterior eye-segment imaging with full-range complex spectral domain optical coherence tomography. J Biomed Opt 2009;14:050501.
18. Grulkowski I, Gora M, Szkulmowski M, et al. Anterior segment imaging with Spectral OCT system using a high-speed CMOS camera. Opt Express 2009;17:4842-58.
19. Chansangpetch S, Nguyen A, Mora M, et al. Agreement of Anterior Segment Parameters Obtained From Swept-Source Fourier-Domain and Time-Domain Anterior Segment Optical Coherence Tomography. Invest Ophthalmol Vis Sci 2018;59:1554-61.
20. Shoji T, Kato N, Ishikawa S, et al. Association between axial length and in vivo human crystalline lens biometry during accommodation: a swept-source optical coherence tomography study. Jpn J Ophthalmol 2020;64:93-101.
21. Xiang Y, Fu T, Xu Q, et al. Quantitative analysis of internal components of the human crystalline lens during accommodation in adults. Sci Rep 2021;11:6688.
22. Mitsukawa T, Suzuki Y, Momota Y, et al. Anterior Segment Biometry During Accommodation and Effects of Cycloplegics by Swept-Source Optical Coherence Tomography. Clin Ophthalmol 2020;14:1237-43.
23. Shoji T, Kato N, Ishikawa S, et al. In vivo crystalline lens measurements with novel swept-source optical coherent tomography: an investigation on variability of measurement. BMJ Open Ophthalmol 2017;1:e000058.
24. Xie X, Sultan W, Corradetti G, et al. Assessing accommodative presbyopic biometric changes of the entire anterior segment using single swept-source OCT image acquisitions. Eye (Lond) 2022;36:119-28.
25. Kimura S, Morizane Y, Shiode Y, et al. Assessment of tilt and decentration of crystalline lens and intraocular lens relative to the corneal topographic axis using anterior segment optical coherence tomography. PLoS One 2017;12:e0184066.
26. Wang L, Jin G, Zhang J, et al. Clinically Significant Intraocular Lens Decentration and Tilt in Highly Myopic Eyes: A Swept-Source Optical Coherence Tomography Study. Am J Ophthalmol 2022;235:46-55.
27. Dubbelman M, Van der Heijde GL. The shape of the aging human lens: curvature, equivalent refractive index and the lens paradox. Vision Res 2001;41:1867-77.
28. Schachar RA, Davila C, Pierscionek BK, et al. The effect of human in vivo accommodation on crystalline lens stability. Br J Ophthalmol 2007;91:790-3.
29. Abolmaali A, Schachar RA, Le T. Sensitivity study of human crystalline lens accommodation. Comput Methods Programs Biomed 2007;85:77-90.
30. Schachar RA, Fygenson DK. Topographical changes of biconvex objects during equatorial traction: an analogy for accommodation of the human lens. Br J Ophthalmol 2007;91:1698-703.
31. Martinez-Enriquez E, Pérez-Merino P, Velasco-Ocana M, et al. OCT-based full crystalline lens shape change during accommodation in vivo. Biomed Opt Express 2017;8:918-33.
32. Pérez-Merino P, Velasco-Ocana M, Martinez-Enriquez E, et al. OCT-based crystalline lens topography in accommodating eyes. Biomed Opt Express 2015;6:5039-54.
33. Dubbelman M, Van der Heijde GL, Weeber HA. Change in shape of the aging human crystalline lens with accommodation. Vision Res 2005;45:117-32.
34. Yuan Y, Chen F, Shen M, et al. Repeated measurements of the anterior segment during accommodation using long scan depth optical coherence tomography. Eye Contact Lens 2012;38:102-8.
35. Gambra E, Ortiz S, Perez-Merino P, et al. Static and dynamic crystalline lens accommodation evaluated using quantitative 3-D OCT. Biomed Opt Express 2013;4:1595-609.
36. Gibson GA, Cruickshank FE, Wolffsohn JS, et al. Optical Coherence Tomography Reveals Sigmoidal Crystalline Lens Changes during Accommodation. Vision (Basel) 2018;2:33.
37. Ruggeri M, de Freitas C, Williams S, et al. Quantification of the ciliary muscle and crystalline lens interaction during accommodation with synchronous OCT imaging. Biomed Opt Express 2016;7:1351-64.

38. Richdale K, Sinnott LT, Bullimore MA, et al. Quantification of age-related and per diopter accommodative changes of the lens and ciliary muscle in the emmetropic human eye. Invest Ophthalmol Vis Sci 2013;54:1095-105.
39. Jaimes-Nájera A, Gómez-Correa JE, Coello V, et al. Single function crystalline lens capable of mimicking ciliary body accommodation. Biomed Opt Express 2020;11:3699-716.
40. Pierscionek BK, Regini JW. The gradient index lens of the eye: an opto-biological synchrony. Prog Retin Eye Res 2012;31:332-49.
41. Khan A, Pope JM, Verkicharla PK, et al. Change in human lens dimensions, lens refractive index distribution and ciliary body ring diameter with accommodation. Biomed Opt Express 2018;9:1272-82.
42. de Castro A, Birkenfeld J, Maceo B, et al. Influence of shape and gradient refractive index in the accommodative changes of spherical aberration in nonhuman primate crystalline lenses. Invest Ophthalmol Vis Sci 2013;54:6197-207.
43. Zhong J, Tao A, Xu Z, et al. Whole eye axial biometry during accommodation using ultra-long scan depth optical coherence tomography. Am J Ophthalmol 2014;157:1064-69.

doi: 10.21037/aes-21-70
Cite this article as: Wang L, Jin G, Ruan X, Gu X, Chen X, Wang W, Dai Y, Liu Z, Luo L. Changes in crystalline lens parameters during accommodation evaluated using swept source anterior segment optical coherence tomography. Ann Eye Sci 2022;7:33.